January 2013

Structural and functional aspects of hetero-oligomers formed by the small heat shock proteins αB-crystallin and HSP27

J Andrew Aquilina
University of Wollongong, aquilina@uow.edu.au

Sudichhya Shrestha
University of Wollongong

Amie M. Morris
University of Wollongong, amorris@uow.edu.au

Heath Ecroyd
University of Wollongong, heathe@uow.edu.au

Structural and functional aspects of hetero-oligomers formed by the small heat shock proteins αB-crystallin and HSP27

Abstract

Small heat shock proteins (sHSPs) exist as large polydisperse species in which there is constant dynamic subunit exchange between oligomeric and dissociated forms. Their primary role *in vivo* is to bind destabilized proteins and prevent their misfolding and aggregation. αB-Crystallin (αB) and HSP27 are the two most widely distributed and most studied sHSPs in the human body. They are coexpressed in different tissues, where they are known to associate with each other to form hetero-oligomeric complexes. In this study, we aimed to determine how these two sHSPs interact to form hetero-oligomers *in vitro* and whether, by doing so, there is an increase in their chaperone activity and stability compared with their homo-oligomeric forms. Our results demonstrate that HSP27 and αB formed polydisperse hetero-oligomers *in vitro*, which had an average molecular mass that was intermediate of each of the homo-oligomers and which were more thermostable than αB, but less so than HSP27. The hetero-oligomer chaperone function was found to be equivalent to that of αB, with each being significantly better in preventing the amorphous aggregation of α-lactalbumin and the amyloid fibril formation of α-synuclein in comparison with HSP27. Using mass spectrometry to monitor subunit exchange over time, we found that HSP27 and αB exchanged subunits 23% faster than the reported rate for HSP27 and αA and almost twice that for αA and αB. This represents the first quantitative evaluation of αB/HSP27 subunit exchange, and the results are discussed in the broader context of regulation of function and cellular proteostasis.

Keywords

heat, shock, proteins, aspects, hetero, structural, oligomers, functional, formed, small, crystallin, hsp27, b

Disciplines

Medicine and Health Sciences

Publication Details

Aquilina, J. Andrew., Shrestha, S., Morris, A. M. & Ecroyd, H. (2013). Structural and functional aspects of hetero-oligomers formed by the small heat shock proteins αB-crystallin and HSP27. Journal of Biological Chemistry, 288 (19), 13602-13609.

Structural and Functional Aspects of Hetero-oligomers Formed by the Small Heat-Shock Proteins αB-crystallin and HSP27

J. Andrew Aquilina, Sudichhya Shrestha, Amie M. Morris, and Heath Ecroyd

Illawarra Health and Medical Research Institute and School of Biological Sciences, University of Wollongong, Wollongong, NSW Australia 2522.

*Running title: *Hetero-oligomers of small heat shock proteins*

To whom correspondence should be addressed: J. Andrew Aquilina, Illawarra Health and Medical Research Institute and School of Biological Sciences, University of Wollongong, Wollongong, NSW Australia, Tel.: +61 (2) 4221-3340; Fax: +61 (2) 4221-810; E-mail: aquilina@uow.edu.au or Heath Ecroyd, Tel.: +61 (2) 4221-3443; Fax: +61 (2) 4221-810; E-mail:heathe@uow.edu.au

Keywords: chaperones; heat shock proteins; mass spectrometry; crystallin, HSP27; aggregation

Background: αB-crystallin and HSP27 are mammalian intracellular small heat-shock proteins.
Results: These proteins exchange subunits in a rapid and temperature dependent manner.
Conclusion: This facile subunit exchange suggests that differential expression could be used by the cell to regulate the response to stress.
Significance: A robust technique defines parameters for the dynamic interaction between the major mammalian small heat-shock proteins.

SUMMARY

Small heat shock proteins (sHSPs) exist as large polydisperse species in which there is constant dynamic subunit exchange between oligomeric and dissociated forms. Their primary role *in vivo* is to bind destabilized proteins and prevent their misfolding and aggregating. αB-Crystallin (αB) and HSP27 are the two most widely distributed and most studied sHSPs in the human body. They are co-expressed in different tissues where they are known to associate with each other and form hetero-oligomeric complexes. This study aimed to determine how these two sHSPs interact to form hetero-oligomers *in vitro* and whether, by doing so, there is an increase in their chaperone activity and stability compared to their homo-oligomeric forms. Results demonstrate that HSP27 and αB form polydisperse hetero-oligomers *in vitro* which have an average molecular mass higher than each of the homo-oligomers and are more thermostable than αB, but less so than HSP27. The hetero-oligomer chaperone function was found to be equivalent to that of αB, with each being significantly better at preventing the amorphous aggregation of α-lactalbumin and the amyloid fibril formation of α-synuclein in comparison to HSP27. Using mass spectrometry to monitor subunit exchange over time it was found that HSP27 and αB exchange subunits 23% faster than the reported rate for HSP27/αA, and almost twice that of αA/αB. This represents the first quantitative evaluation of HSP27/αB subunit exchange and the results are discussed in the broader context of regulation of function and cellular proteostasis.

Incorrect folding (misfolding) of proteins is associated with protein malfunctioning and aggregation (1). Protein aggregation either occurs through disordered (amorphous) and ordered (amyloid fibril) pathways, both of which are nucleation-dependent and lead to the deposition of protein inclusions in cells and tissues (2). The aggregates formed (and in particular fibrils) can be detrimental to cells and tissues and have been associated with a variety of diseases some of the most notable being the neurodegenerative disorders Alzheimer's disease, Parkinson's disease and Huntington's disease (3-5). To prevent protein aggregation the cell employs quality control machinery that acts to encourage protein folding and discourage misfolding (3,4). This quality control machinery therefore acts to maintain protein homeostasis (proteostasis), a process that relies heavily on molecular chaperone and protein degradation systems (6,7).

Heat shock proteins (HSPs) are abundant intracellular chaperones, whose expression is strongly induced in response to physicochemical stresses (7) so that the manifold protein folding events of the cell are maintained. Heat shock proteins are classified into five main families, based on the approximate molecular masses of their monomeric forms: the small heat shock proteins (sHSPs), HSP60, HSP70, HSP90 and HSP100 (7,8). The sHSPs are defined by a conserved α-crystallin domain (of approximately 90 amino acids in length), which is flanked by a

relatively hydrophobic N-terminal domain and a highly polar C-terminal extension (2,9-11).

The sHSPs act by recognising partially-folded protein intermediates that leave the folding/unfolding pathway and enter one of the two off-folding pathways (2). They act to minimise hydrophobic interactions between these intermediates in order to prevent aggregation and subsequent precipitation of the protein. The sHSPs are so named due to the relatively modest masses of their constituent subunits (12 – 42 kDa) (12). Typically, however, sHSPs do not exist as monomers; instead they form large multi-subunit oligomers up to a MDa in mass (13,14) which, in mammals, can also be polydisperse (15). The oligomers formed by sHSPs are dynamic (15-18); they undergo constant subunit exchange and their average size and substructure can be manipulated within the cell, e.g. by phosphorylation (19-22), in order to cater for the various demands placed upon them by a wide variety of target proteins which become destabilised by cellular stressors (23). Thus, oligomer plasticity is an essential feature of sHSPs, however, this has hampered efforts at revealing their structure by crystallography.

The currency of sHSP subunit exchange is thought to be a dimer, as this is a defined unit of symmetry in the monodisperse sHSPs that have had their crystal structure solved (9,24,25). This is also supported by recent crystallographic studies of discrete mammalian sHSP α-crystallin domains, along with a full-length α-crystallin structure solved via a combination of solid-state NMR and small angle X-ray scattering experiments (26-28). However, since mammalian sHSPs can also form oligomers with an odd number of subunits (15,19), it stands to reason that monomers are the fundamental unit of polydisperse sHSPs interactions. This was recently confirmed and formalized in an elegant model of αB-crystallin (αB) quaternary dynamics whereby the entire oligomeric distribution can be described by just two monomer-level interactions (29).

Whilst much work has focussed on the structure and function of homo-oligomeric forms of sHSPs, *in vivo* sHSPs are thought to predominately exist as hetero-oligomers. This is particularly evident in the eye lens where heterogeneous multimers of αA-crystallin (αA) and αB make up α-crystallin, the major crystallin protein found in this tissue (2,30,31). Previous studies have reported the co-localisation of HSP27 and αB in both normal tissue (e.g. kidneys, bladder, lungs, stomach, cardiac and skeletal muscle (32,33) and pathological tissues of neurodegenerative patients (32,34). The sHSPs have been shown to partially associate with each other in these tissues (32,35) and have been shown to form hetero-oligomers *in vitro* (17,36). Therefore, a better understanding of the structural and functional characteristics of the HSP27 and αB hetero-oligomeric complexes is clearly warranted.

In the present work we demonstrate that HSP27 and αB readily form mixed oligomers *in vitro*, and that this process of subunit exchange occurs rapidly at physiological temperature. The size of the hetero-oligomers thus formed was found to be intermediate between the homo-oligomeric assemblies, as was their relative stability to heat stress. Functional assays revealed that αB was the determining factor in suppressing both amorphous and fibrillar aggregation in our model systems, as HSP27 alone was an inferior chaperone. Finally, using mass spectrometry, we describe in detail, the temperature dependent subunit exchange kinetics between HSP27 and αB; the first such study to address this important physiologically relevant interaction.

EXPERIMENTAL PROCEDURES

Materials–All biochemicals and reagents used were of analytical grade and purchased from Sigma-Aldrich (St. Louis, MO, USA) unless otherwise specified. Dithiothreitol (DTT) was obtained from Astral Scientific (Sydney, NSW, Australia), ampicillin and kanamycin were obtained from Amresco (Solon, OH, USA). Human αB in the pET24d (+) vector and HSP27 in pET 3a vector (Novagen, SanDiego, CA, USA), were donated by Drs. W. De Jong and W. Boelens (University of Nijmegen, Netherlands). Plasmids were transformed into competent *Escherichia coli* (*E. coli*) strain BL21 (DE3) cells using standard techniques and expressed and purified as described previously (37). The concentrations of proteins used in this study were determined using the following absorption extinction coefficients (ε280 nm of a 0.1% w/v solution, mL. $mg^{-1}.cm^{-1}$) and calculated molecular masses (in kDa): α-lactalbumin (2.09, 14.20) (38); α-synuclein (0.35, 14.46) (39); HSP27 (1.65, 22.78) (40); αB (0.83, 20.15) (38).

SDS-PAGE and Native PAGE–SDS-PAGE was performed on discontinuous polyacrylamide gels using a 4% (v/v) stacking gel and 12% (v/v) resolving gel and standard techniques as per the manufacturer's recommendations (Bio-Rad, Hercules, CA, USA). Native-PAGE was performed on discontinuous polyacrylamide gels using a 4% (v/v) stacking gel and 6% (v/v) resolving gel according to the method of (41).

Size, polydispersity and thermal stability of the oligomeric complexes–In order to investigate the size of homo- and hetero-oligomeric complexes of αB and HSP27 dynamic light scattering (DLS) was performed. Samples of HSP27, αB and an equimolar mixture of the two were prepared in 50 mM phosphate buffer containing 100 mM NaCl (pH 7.0) at a final concentration of 50 μM and incubated at 37°C for 1 h in order to initiate subunit exchange. Samples were then placed on ice which halts

further subunit exchange (15). DLS was performed using a Malvern Zetasizer auto-plate sampler (APS) system (Malvern Instruments, Worcestershire, UK). Samples (60 µL) were aliquoted into wells of a 96-well microtitre plate which was held at 4ºC. Measurements were performed at 37ºC following a 30 s equilibration time. Accumulation times for each sample were determined automatically using the inbuilt software and the correlogram used to calculate the hydrodynamic diameter (nm) and estimate the polydispersity of the particles in solution. The thermal stability of the oligomers was measured using the temperature melt trend function of the Malvern APS system. The temperature was increased from 25ºC to 80ºC (in 1ºC increments) and the melting temperature (Tm) was taken to be the temperature at which the hydrodynamic diameter of the protein had increased 2-fold from that measured at 25 ºC. All experiments were repeated three times and results shown are a representative of these experiments.

Aggregation assays–Experiments were performed to investigate the relative chaperone activity of homo- and hetero-oligomeric complexes of HSP27 and αB against both amorphous and amyloid fibril type aggregation. At the end of each assay (i.e. 12.5 h for the α-lactalbumin assay and 50 h for the α-synuclein assay), the ability of the sHSPs to inhibit protein aggregation was determined by calculating the percent protection using the formula:

$$\% \text{ protection} = 100 \times (\Delta Ic - \Delta Is)/\Delta Ic$$

where, ΔIc and ΔIs represent the change in absorbance (A360) or thioflavin T (ThT) fluorescence for the target protein in the absence or presence of chaperones, respectively. All assays were repeated at least three times. Results shown are the changes in light scatter at 360 nm, or ThT fluorescence, over time for one representative experiment. For percent protection afforded by the chaperones, results are mean ± SEM of the three independent experiments. Data were subsequently analyzed using a one-way ANOVA and differences between treatments were established with Tukey's post-hoc test using GraphPad Prism 5.01. Values of $p < 0.05$ were considered significant.

Reduction-induced amorphous aggregation of α-lactalbumin–Bovine milk α-lactalbumin (100 µM) was incubated in 50 mM phosphate buffer containing 100 mM NaCl and 2 mM EDTA (pH 7.0) at 37°C for 10 h in the absence or presence of sHSPs at molar ratios between 16:1 to 2:1 (α-lactalbumin:sHSPs). In experiments performed with an equimolar mixture of the two sHSPs, the concentration of each individual sHSP was halved so that the final concentration of the hetero-oligomers was the same as that of the homo-oligomers. Samples were prepared in duplicate in Greiner 96 well microplates (100 µL/well) (Greiner Bio-One, Monroe, NC, USA) and the aggregation of α-lactalbumin was initiated by addition of 20 mM DTT (Horwitz, 2005). The plates were sealed with SealPlate film (Sigma-Aldrich, St. Louis, MO, USA) to prevent evaporation. The precipitation of α-lactalbumin was monitored via light scattering at 360 nm using a FLUOstar OPTIMA plate reader (BMG Lab technologies, Melbourne, VIC, Australia). Samples were shaken for 30 s prior to the first absorbance reading and measurements were made every 3 min for 720 min.

Amyloid fibril aggregation of α-synuclein–The formation of amyloid fibrils by α-synuclein was measured using a ThT fluorescence assay adapted from Rekas *et al.* (42). Briefly, α-synuclein (125 µM) in 50 mM phosphate buffer containing 100 mM NaCl (pH 7.4), was incubated in the absence or presence of αB, HSP27 or an equimolar mixture of the two such that the molar ratios tested ranged from 1:0.05 to 1:0.1 (α-synuclein:sHSPs). Samples were prepared in duplicate and incubated with 10 µM ThT in Greiner 384 well microplates to a final volume of 50 µL/well (Greiner Bio-One, Monroe, NC, USA). The plates were sealed with SealPlate film (Sigma-Aldrich, St. Louis, MO, USA) and incubated at 37°C for 50 h, with 5 min shaking after every fluorescence reading. The change in ThT fluorescence intensity (excitation 440 nm, emission 490 nm) was monitored at intervals of 12 min for 3000 min using a Polarstar Optima plate reader (BMG Lab technologies, Melbourne, VIC, Australia).

Subunit exchange and mass spectrometry–Approximately 2 mg of the purified and concentrated proteins (25 mg/ml) were buffer-exchanged by loading onto a Superdex™ 200 10/300 GL column and eluting at 0.3 mL/min with 200 mM NH_4OAc. A 0.3 mL fraction corresponding to the apex of the A^{280} chromatogram for each sHSP was collected for use in all subunit exchange experiments. Subunit exchange reactions were performed in Eppendorf tubes in a temperature-controlled water bath at 23°C, 30°C and 37°C. Protein concentrations were 20 µM HSP27 and 10 µM αB in 50 µL of 200 mM NH_4OAc, 1 mM DTT at time zero. 5 µL volumes of sample were taken at regular time intervals during the exchange and immediately put on ice prior to analysis. Nanoelectrospray mass spectrometry was performed using a SYNAPT G2 HDMS spectrometer (Waters, UK) in positive ion mode with the following instrument conditions: capillary, 1.6 kV; sample cone, 200 V; extractor, 10 V; trap collision energy, 80 V; transfer collision energy, 180 V. Argon gas was introduced into the collision cell at 9.0 mL/min to promote the dissociation of monomers from the hetero-oligomeric assemblies. The pressures in the various stages of the instrument were as follows: Backing, 7.3

mbar; Trap, 3.8 x 10^{-2} mbar; IM, 2.66 x 10^{-2} mbar; ToF, 2.2 x 10^{-6} mbar. All spectra were externally calibrated using a solution of cesium iodide (10 mg/mL in water) and processed post-acquisition using Masslynx 4.1 software (Waters, UK). Kinetic data were extracted from the mass spectra by summing the homo-oligomer signature peak intensities, and plotting these values on a log_e scale, versus time. The intensity data (I) were fitted to the exponential function $I(t) = I_0 e^{-kt}$, where k is the subunit exchange rate constant.

RESULTS

Native gel electrophoresis confirmed that HSP27 and αB form hetero-oligomeric complexes *in vitro* (Figure 1A). The absence of individual bands corresponding to homo-oligomeric αB or HSP27 in the lane containing an equimolar mixture of the two indicated that significant subunit exchange had occurred during 60 min incubation at 37ºC. To ascertain if the transition from homo- to hetero-oligomer affected the size of the protein assemblies, we used dynamic light scattering (DLS) to determine their hydrodynamic diameter (Figure 1B). Thus, the hetero-oligomers were found to have a hydrodynamic diameter intermediate between the (smaller) αB and (larger) HSP27 homo-oligomers.

The relative stability of the sHSPs was assessed using dynamic light scattering to monitor particle size in solution (i.e. Z-average) with increasing temperature (Figure 1C). An exponential increase in the Z-average hydrodynamic diameter of the αB homo-oligomers commenced at 60ºC. HSP27 exhibited greater thermo-stability than αB, with the increase in the Z-average not occurring until 68ºC, while the hetero-oligomers had a melting temperature that was intermediate to the homo-oligomeric forms; the increase in particle size occurring at 64ºC.

Reduction-induced amorphous aggregation of α-lactalbumin was used to assess the chaperone efficiency of the sHSPs against amorphously aggregating target proteins as this is an established model, and is conducted under conditions of physiological temperature and pH. In the absence of sHSPs, aggregation of α-lactalbumin commenced after 15 min and rapidly increased until it reached a plateau at approximately 250 min (Figure 2A). In the presence of sHSPs, there was an increase in the time before aggregation commenced (i.e. lag phase) and an overall reduction in the light scattering associated with α-lactalbumin aggregation. There was no change in light scattering when the buffer and sHSPs were incubated in the absence of α-lactalbumin indicating that the increase in light scatter was associated with the aggregation of α-lactalbumin. Overall, there was a concentration-dependent increase in the protection afforded by the homo- and hetero-oligomeric sHSPs, demonstrating that these related sHSP species commingle rather than form self-chaperoning complexes. αB homo-oligomers and the αB/HSP27 hetero-oligomers were significantly more effective at inhibiting α-lactalbumin aggregation than HSP27 homo-oligomers at molar ratios of 4:1, 8:1 and 16:1 (α-lactalbumin: sHSPs) (Figure 2B). However, there was no significant difference in chaperone activity between the αB homo-oligomers or hetero-oligomers at these molar ratios.

A thioflavin T (ThT) binding assay was used to assess the chaperone efficacy of the sHSPs against α-synuclein amyloid fibril type aggregation. This is a disease based model that is physiologically relevant as the *in vivo* aggregation occurs inside cells. In the absence of sHSP, ThT fluorescence associated with α-synuclein fibril formation was observed to increase from 15 h and continue rising over the remaining 35 h of the assay (Figure 2C). The inclusion of HSP27 at a 10:1 molar ratio (α-synuclein: sHSP) resulted in a modest reduction in fluorescence, however the onset of fibril formation and kinetics of propagation was similar to the control. αB homo-oligomers and the αB/HSP27 hetero-oligomers had a much more pronounced effect on the kinetics of α-synuclein fibril formation. Firstly, there was a significant increase in the lag phase of the aggregation, extending to 36 h compared to the 15 h lag phase for HSP27. Secondly, there was an 80% reduction in ThT fluorescence after 50 h compared with the control, demonstrating superior efficacy over HSP27 homo-oligomers (which only reduced ThT fluorescence by 32%). There was no change in ThT fluorescence when the buffer and sHSPs were incubated in the absence of α-synuclein.

At molar ratios of 10:1 and 20:1 (α-synuclein:sHSP) homo-oligomeric αB and αB/HSP27 hetero-oligomers were significantly more effective at inhibiting α-synuclein fibril formation than HSP27 (Figure 2D). There was no difference in the chaperone activity between the αB homo-oligomers and αB/HSP27 hetero-oligomers at these molar ratios; both suppressed the increase in ThT fluorescence associated with α-synuclein fibril formation by ~85%.

Subunit Exchange–While native PAGE of the αB/HSP27 mixed oligomers provided evidence that these sHSPs were able to exchange subunits (Figure 1A), it revealed little about the kinetics or the extent of hetero-oligomerization. To address these parameters in some detail, we employed nanoelectrospray-ionization mass spectrometry (nanoESI-MS), a technique which is well established for the analysis of polydisperse protein assemblies and their subunit exchange (43). The method developed to monitor subunit exchange exploits the phenomena of

asymmetric dissociation and charge-stripping, which take place in the trap region of the spectrometer. For the purposes of the present study, neutral gas pressure and accelerating potential across the trap were adjusted to promote the removal of up to three monomers from the sHSP assemblies prior to their detection in the time-of-flight tube.

Dissociation spectra for HSP27 and αB homo-oligomers were acquired (Figure 3A), and the *m/z* regions corresponding to oligomers from which monomers have been stripped, are labelled. A notable difference between the spectra of HSP27 and αB was the more facile removal of monomers from αB under identical instrument conditions. The most abundant signal in the HSP27 spectrum arose from oligomers stripped of one monomer (*n-1*), with smaller populations of non-stripped (*n*) and oligomers stripped of two monomers (*n-2*) also present. αB, however, had no intact oligomers remaining, and the majority of signal was centred around the *n-2* oligomers. Therefore, under the same conditions, it was possible to remove, on average, one additional αB subunit from its homo-oligomers compared to HSP27.

The *n-2* region is particularly useful in the analysis of polydisperse proteins, as it includes a "signature" peak at an *m/z* value equal to the mass of a single subunit. This unique feature arises from the fact that for all oligomers in the polydisperse assembly, when the number of subunits is equal to the number of charges, i.e., n^{n+}, the resulting ions overlap at the signature peak *m/z* value (43). This singularity has the effect of greatly simplifying the *n-2* region, as shown for αB and HSP27 (Figures 3B and C). Consequently, it is relatively straightforward to assign this region of the spectrum for a polydisperse protein, as indicated by the labelled ions in these spectra. For αB, the major oligomers were found to range in size from 18 to 30 subunits [(*n-2)* + 2], with those containing an even number of subunits dominating the distribution (Figure 3B). HSP27 had the same range of oligomers as αB, however the distribution was significantly skewed due to a high proportion of signal arising from 20- and 22-mers.

This clear separation of αB and HSP27 signature peaks on the *m/z* scale allowed us to examine the solution phase subunit exchange reaction between these two sHSPs. Mixtures were incubated at 23, 30 or 37°C and spectra acquired at regular time intervals to monitor the extent of hetero-oligomerization. Data for the 30°C reaction mixture, acquired over a period of 30 min are presented in Figure 4A. As subunit exchange proceeded, a peak corresponding to the formation of a hetero-oligomeric product was observed to emerge at ~*m/z* 22400. This was accompanied by a minor decay in the relative intensities of the signature peaks, however, unlike exchange reactions between αA- and αB (43), there was negligible shift in the *m/z* values of these peaks. This implies that the subunit exchange between αB and HSP27 does not proceed uniformly throughout the system, but rather, a subpopulation of oligomers participates preferentially to the remaining non-exchanged homo-oligomers.

As noted above, the hetero-oligomer signature peak emerged at ~*m/z* 22400, a value much higher than that expected for a fully exchanged αB/HSP27 species. The homo-oligomer concentrations used in these experiments were 10 μM (αB) and 20 μM (HSP27), which, if fully and freely exchanged would generate hetero-oligomers with a signature peak at ~*m/z* 21850; i.e. 550 *m/z* units less than the species observed (Figure 4A). We investigated this disparity by examining the mass spectra acquired after greater periods of subunit exchange. Although the signal to noise ratio of the data decreased significantly with time, we were in fact able to observe a broad peak centred at *m/z* 21900 after 75 min (Figure 4B), indicating that complete exchange does eventuate. For each of the reaction temperatures, the subunit exchange rate constant (*k*) was obtained by plotting the homo-oligomer intensities versus time (Figure 4C) and determined to be: $k_{23} = 2.0\times10^{-3}$ min^{-1}; $k_{30} = 1.4\times10^{-2}$ min^{-1}; $k_{37} = 7.1\times10^{-2}$ min^{-1}.

DISCUSSION

The hetero-oligomeric α-crystallin of the eye lens is massively abundant at a ratio of approximately three αA subunits to one αB. While αB is also widely distributed throughout the body, αA is virtually confined to lenticular fiber cells. Considering that HSP27 and αB are known to co-localize in many tissues, including skeletal muscle, this points to HSP27 being the extra-lenticular compeer of αB. However, whilst the interactions between αA and αB have been exhaustively examined, the literature regarding mixed assemblies of HSP27 and αB is scant. In the present study, we have endeavoured to address this deficiency by characterizing some key functional and structural aspects of HSP27 and αB hetero-oligomerization.

In agreement with previous work (36,44), HSP27 and αB were able to form hetero-oligomeric complexes *in vitro*. Thus, native-PAGE showed a single diffuse band when HSP27 and αB were mixed, indicative of the comprehensive dynamic subunit exchange that is typical of mammalian sHSPs (17,45), along with the well-known polydispersity of mammalian sHSPs. Furthermore, these complexes exhibited an amalgamation of structural and functional characteristics derived from the homo-oligomeric populations. For example, the hetero-oligomers had a size and thermal stability midway between the homo-oligomeric forms. The functional efficiencies of the hetero-oligomeric complexes

was assessed using target proteins that aggregate either amorphously (α-lactalbumin) or to form disease-associated amyloid fibrils (α-synuclein). In both cases the hetero-oligomers were equivalent in their chaperone capacity to αB homo-oligomers, and superior to HSP27 homo-oligomers. Thus, our data suggests that it is advantageous for HSP27 and αB to form hetero-oligomeric complexes: HSP27 would stabilise αB in tissues in which they are co-expressed (as αA does in the eye lens) and the chaperone activity is as good as (or, in the case of HSP27, better than) the homo-oligomeric forms.

Though it is well established that HSP27and αB can form mixed assemblies when incubated *in vitro*, it is important to understand the kinetics of the subunit exchange process in order to determine if the time-scale is relevant to their *in vivo* expression. Subunit exchange studies using fluorescence resonance energy transfer (FRET) at 37°C have been reported for HSP27/αA and αA/αB (17), with rate constants of 5.76×10^{-2} min^{-1} and 3.78×10^{-2} min^{-1} respectively. These FRET studies depend upon the attachment of a fluorescent probe to a free cysteine under basic conditions for several hours, which, while not structurally destructive, has the potential to alter the dynamics of subunit exchange. For example, we have observed relatively high levels of disulfide linked dimers in the mass spectrum of HSP27 expressed in *E. coli*, while *in vivo,* these dimers have been observed to account for more than 50 per cent of total HSP27 in SH-SY5Y cells expressing the protein. (46). These researchers suggested that the ratio between monomeric and dimeric HSP27 is a key determinant for the activity of the protein. In this context, FRET experiments, which rely on the attachment of fluorophores to Cys residues, preclude the formation of HSP27 (and αA) dimers, thereby excluding this major parameter from the system. As noted above, our recombinant HSP27 was a mixture of disulfide-linked dimers and monomers after purification, however for this initial work, and to facilitate comparison with previously published studies, we reduced all disulfides in HSP27 prior to use.

Using nanoelectrospray mass spectrometry, we were able to monitor (in real-time) the subunit exchange between native label-free HSP27 and αB. Both proteins are broadly distributed in mammalian tissue and over-expressed under stress conditions; thus, a description of the process(es) leading to hetero-complex formation is germane. At 37°C, the exchange rate constant was found to be 7.1×10^{-2} min^{-1}, which is 23% faster than the HSP27/αA rate, and almost twice that of αA/αB exchange at the same temperature previously reported (17). Considering the relatively static environment of the lens, it is not surprising that α-crystallin subunit exchange is less vigorous, however it should be emphasized that modulation of sHSP interactions via HSP27 phosphorylation and disulphide redox, may provide considerable dynamic range to the system. For example, the triple serine to aspartate phosphomimic of HSP27 is a discrete dimer (40,47,48), which *in vitro* at least, is a superior chaperone to the larger oligomers (18). Therefore, *in vivo*, one may envisage a complex matrix of hetero-oligomeric permutations, which, coupled with highly dynamic subunit exchange, perform multifarious roles in the cell. Conversely, it may be that the overproduction of sHSP species with enhanced or inappropriate chaperone activity leads to co-localized deposition of sHSPs in some pathologies. Currently, the characteristics of polydisperse and hetero-oligomeric sHSPs are unknown, which presents an exciting area of protein homeostasis to explore.

REFERENCES

1. Dobson, C. M. (2003) *Nature* **426**, 884-890
2. Ecroyd, H., and Carver, J. A. (2009) *Cell Mol Life Sci* **66**, 62-81
3. Chiti, F., and Dobson, C. M. (2006) *Annu Rev Biochem* **75**, 333-366
4. Dobson, C. M. (2001) *Philos Trans R Soc Lond B Biol Sci* **356**, 133-145
5. Muchowski, P. J. (2002) *Neuron* **35**, 9-12
6. Muchowski, P. J., and Wacker, J. L. (2005) *Nat Rev Neurosci* **6**, 11-22
7. Hartl, F. U., Bracher, A., and Hayer-Hartl, M. (2011) *Nature* **475**, 324-332
8. Voisine, C., Pedersen, J. S., and Morimoto, R. I. (2010) *Neurobiol Dis* **40**, 12-20
9. Stamler, R., Kappe, G., Boelens, W., and Slingsby, C. (2005) *J Mol Biol* **353**, 68-79
10. Sun, Y., and MacRae, T. H. (2005) *Cell Mol Life Sci* **62**, 2460-2476
11. de Jong, W. W., Leunissen, J. A., and Voorter, C. E. (1993) *Mol Biol Evol* **10**, 103-126
12. de Jong, W. W., Caspers, G. J., and Leunissen, J. A. (1998) *Int J Biol Macromol* **22**, 151-162
13. Haley, D. A., Bova, M. P., Huang, Q. L., McHaourab, H. S., and Stewart, P. L. (2000) *J Mol Biol* **298**, 261-272
14. Haley, D. A., Horwitz, J., and Stewart, P. L. (1998) *J Mol Biol* **277**, 27-35
15. Aquilina, J. A., Benesch, J. L., Bateman, O. A., Slingsby, C., and Robinson, C. V. (2003) *Proc Natl Acad Sci U S A* **100**, 10611-10616
16. Bova, M. P., Ding, L. L., Horwitz, J., and Fung, B. K. (1997) *J Biol Chem* **272**, 29511-29517
17. Bova, M. P., McHaourab, H. S., Han, Y., and Fung, B. K. (2000) *J Biol Chem* **275**, 1035-1042
18. Shashidharamurthy, R., Koteiche, H. A., Dong, J., and McHaourab, H. S. (2005) *J Biol Chem* **280**, 5281-5289
19. Aquilina, J. A., Benesch, J. L., Ding, L. L., Yaron, O., Horwitz, J., and Robinson, C. V. (2004) *J Biol Chem* **279**, 28675-28680
20. Ecroyd, H., Meehan, S., Horwitz, J., Aquilina, J. A., Benesch, J. L., Robinson, C. V., Macphee, C. E., and Carver, J. A. (2007) *Biochem J* **401**, 129-141
21. Ito, H., Kamei, K., Iwamoto, I., Inaguma, Y., Nohara, D., and Kato, K. (2001) *J Biol Chem* **276**, 5346-5352
22. Kato, K., Hasegawa, K., Goto, S., and Inaguma, Y. (1994) *J Biol Chem* **269**, 11274-11278
23. Stengel, F., Baldwin, A. J., Painter, A. J., Jaya, N., Basha, E., Kay, L. E., Vierling, E., Robinson, C. V., and Benesch, J. L. (2010) *Proc Natl Acad Sci U S A* **107**, 2007-2012
24. Kim, K. K., Kim, R., and Kim, S. H. (1998) *Nature* **394**, 595-599
25. van Montfort, R. L., Basha, E., Friedrich, K. L., Slingsby, C., and Vierling, E. (2001) *Nat Struct Biol* **8**, 1025-1030
26. Jehle, S., Rajagopal, P., Bardiaux, B., Markovic, S., Kuhne, R., Stout, J. R., Higman, V. A., Klevit, R. E., van Rossum, B. J., and Oschkinat, H. (2010) *Nat Struct Mol Biol* **17**, 1037-1042
27. Jehle, S., van Rossum, B., Stout, J. R., Noguchi, S. M., Falber, K., Rehbein, K., Oschkinat, H., Klevit, R. E., and Rajagopal, P. (2009) *J Mol Biol* **385**, 1481-1497
28. Laganowsky, A., Benesch, J. L., Landau, M., Ding, L., Sawaya, M. R., Cascio, D., Huang, Q., Robinson, C. V., Horwitz, J., and Eisenberg, D. (2010) *Protein Sci* **19**, 1031-1043
29. Baldwin, A. J., Lioe, H., Robinson, C. V., Kay, L. E., and Benesch, J. L. (2011) *J Mol Biol* **413**, 297-309
30. Bloemendal, H., de Jong, W., Jaenicke, R., Lubsen, N. H., Slingsby, C., and Tardieu, A. (2004) *Prog Biophys Mol Biol* **86**, 407-485
31. Horwitz, J. (2000) *Semin Cell Dev Biol* **11**, 53-60
32. Kato, K., Shinohara, H., Goto, S., Inaguma, Y., Morishita, R., and Asano, T. (1992) *J Biol Chem* **267**, 7718-7725
33. Sakuma, K., Watanabe, K., Totsuka, T., and Kato, K. (1998) *Biochim Biophys Acta* **1406**, 162-168
34. Arrigo, A. P., Simon, S., Gibert, B., Kretz-Remy, C., Nivon, M., Czekalla, A., Guillet, D., Moulin, M., Diaz-Latoud, C., and Vicart, P. (2007) *FEBS letters* **581**, 3665-3674

35. Zantema, A., Verlaan-De Vries, M., Maasdam, D., Bol, S., and van der Eb, A. (1992) *J Biol Chem* **267**, 12936-12941
36. Fontaine, J. M., Sun, X., Benndorf, R., and Welsh, M. J. (2005) *Biochemical and biophysical research communications* **337**, 1006-1011
37. Horwitz, J., Huang, Q. L., Ding, L., and Bova, M. P. (1998) *Methods Enzymol* **290**, 365-383
38. Pace, C. N., Vajdos, F., Fee, L., Grimsley, G., and Gray, T. (1995) *Protein Sci* **4**, 2411-2423
39. Narhi, L., Wood, S. J., Steavenson, S., Jiang, Y., Wu, G. M., Anafi, D., Kaufman, S. A., Martin, F., Sitney, K., Denis, P., Louis, J. C., Wypych, J., Biere, A. L., and Citron, M. (1999) *J Biol Chem* **274**, 9843-9846
40. Hayes, D., Napoli, V., Mazurkie, A., Stafford, W. F., and Graceffa, P. (2009) *J Biol Chem* **284**, 18801-18807
41. Cassiman, J. J., Marynen, P., Brugmans, M., Van Leuven, F., and Van den Berghe, H. (1981) *Cell Biol Int Rep* **5**, 901-911
42. Rekas, A., Adda, C. G., Aquilina, J. A., Barnham, K. J., Sunde, M., Galatis, D., Williamson, N. A., Masters, C. L., Anders, R. F., Robinson, C. V., Cappai, R., and Carver, J. A. (2004) *J Mol Biol* **340**, 1167-1183
43. Aquilina, J. A., Benesch, J. L., Ding, L. L., Yaron, O., Horwitz, J., and Robinson, C. V. (2005) *J Biol Chem* **280**, 14485-14491
44. Fu, L., and Liang, J. J. (2003) *Biochemical and biophysical research communications* **302**, 710-714
45. Sobott, F., Benesch, J. L., Vierling, E., and Robinson, C. V. (2002) *J Biol Chem* **277**, 38921-38929
46. Almeida-Souza, L., Goethals, S., de Winter, V., Dierick, I., Gallardo, R., Van Durme, J., Irobi, J., Gettemans, J., Rousseau, F., Schymkowitz, J., Timmerman, V., and Janssens, S. (2010) *J Biol Chem* **285**, 12778-12786
47. Lambert, H., Charette, S. J., Bernier, A. F., Guimond, A., and Landry, J. (1999) *J Biol Chem* **274**, 9378-9385
48. McDonald, E. T., Bortolus, M., Koteiche, H. A., and McHaourab, H. S. (2012) *Biochemistry* **51**, 1257-1268

FOOTNOTES

*This work was supported by NHMRC grant 514615 to JAA. HE is the recipient of an ARC Future Fellowship (FT110100586).

FIGURE LEGENDS

FIGURE 1: HSP27 and αB form hetero-oligomeric complexes *in vitro*. **(A)** Discontinuous native-PAGE analysis of αB, HSP27 and an equimolar mixture of the two. The intermediate migration position of the mixture indicates that significant subunit exchange had occurred. **(B)** Dynamic light scattering measurements demonstrated that when mixed, αB (blue) and HSP27 (red) form a polydisperse population (gold) with a size distribution intermediate to the two homo-oligomers. **(C)** Thermal denaturation curves for αB (blue), HSP27 (red) and an equimolar mixture of the two (gold). The change in average particle size (Z-average), as measured by dynamic light scattering, was used to estimate protein aggregation as the temperature was increased by 1°C/min from 25 to 95°C. Results shown are representative of three independent experiments.

FIGURE 2: The chaperone activity of hetero-oligomeric complexes formed between αB and HSP27. The ability of the homo- and hetero-oligomers to prevent the **(A and B)** reduction-induced amorphous aggregation of bovine α-lactalbumin, and **(C and D)** amyloid fibril formation of α-synuclein was examined. A representative trace showing the change in (A) light scatter at 360 nm or (C) ThT fluorescence emission at 490 nm, in the absence (purple) or presence of HSP27 (red), αB (blue), or an equimolar mixture of the two (gold) is shown. Molar ratios shown are 8:1 (α-lactalbumin:sHSP) or 10:1 (α-synuclein:sHSP). Samples containing αB (orange) or HSP27 (grey) alone, overlap at the bottom of the trace. (B and D) The percent protection afforded by the sHSPs at the various molar ratios (target protein:sHSP) tested. Results shown are mean ± SEM of four independent experiments. * denotes a significant ($p<0.05$) difference compared to the αB and mixed oligomers at the same molar ratio.

FIGURE 3: Dissociation mass spectrometry of HSP27 and αB. **(A)** By careful selection of accelerating voltages across, and argon gas flow into, the collision cell, it was possible to remove two and three monomers from the hetero-oligomeric assemblies of HSP27 and αB, respectively. In the region of the spectrum assigned to the doubly stripped oligomers (*n*-2), the peaks were sufficiently resolved such that assignments to individual oligomers could be made. **(B and C)** Expanded view of charge state clusters either side of the major overlapping peaks in the *n*-2 region of αB and HSP27 respectively. Charge state assignments were used to define the range of oligomers present in these sHSPs corresponding to the SEC peak maxima fractions.

FIGURE 4: Monitoring subunit exchange at 30°C using mass spectrometry. **(A)** Doubly stripped oligomer region of the mass spectra for a mixture of HSP27 and αB was monitored over a 30 min period. A peak corresponding to the formation of hetero-oligomer was observed to emerge at ~*m/z* 22400, accompanied by a minor decay in the relative intensities of the homo-oligomer signature peaks at ~*m/z* 20160 (αB), and ~*m/z* 22700 (HSP27). The genesis and progression of the hetero-oligomer peak indicates that exchange occurs predominantly via incorporation of αB subunits into HSP27 oligomers. The 30 min time point spectrum is colored for contrast. **(B)** Monitoring the reaction for a sufficient period of time demonstrates that there is complete exchange of subunits between HSP27 and αB. The spectra are colored to distinguish overlapping traces. **(C)** Subunit exchange kinetics of HSP27 and αB as a function of temperature. Logarithmic plots of homo-oligomer decay versus time at 37°C (red circles), 30°C (yellow squares) and 23°C (blue diamonds), demonstrating a linear relationship, and therefore a first order type reaction. Rate constants for subunit exchange at each temperature were determined from the slope of the corresponding plot.

Figure 1

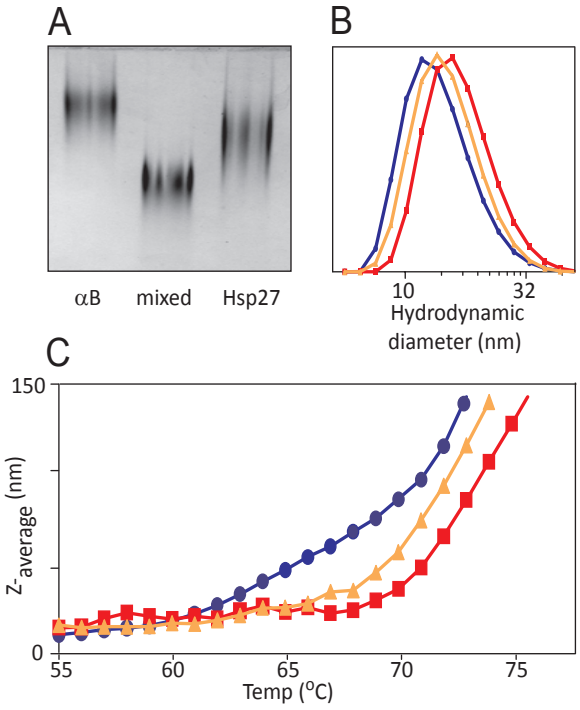
A
αB
mixed
Hsp27
B
10
32
Hydrodynamic
diameter (nm)
C
150
0
Z-average (nm)
55
60
65
70
75
Temp (°C)

Figure 2

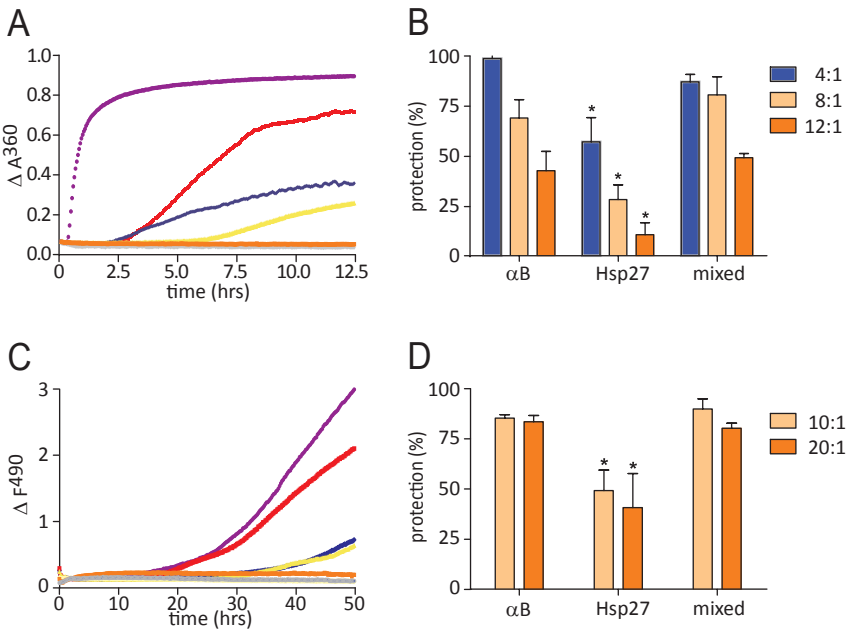
A
1.0
0.8
0.6
0.4
0.2
0.0
Δ A360
0
2.5
5.0
7.5
10.0
12.5
time (hrs)
B
100
75
50
25
0
protection (%)
*
*
*
αB
Hsp27
mixed
4:1
8:1
12:1
C
3
2
1
0
Δ F490
0
10
20
30
40
50
time (hrs)
D
100
75
50
25
0
protection (%)
*
*
αB
Hsp27
mixed
10:1
20:1

Figure 3

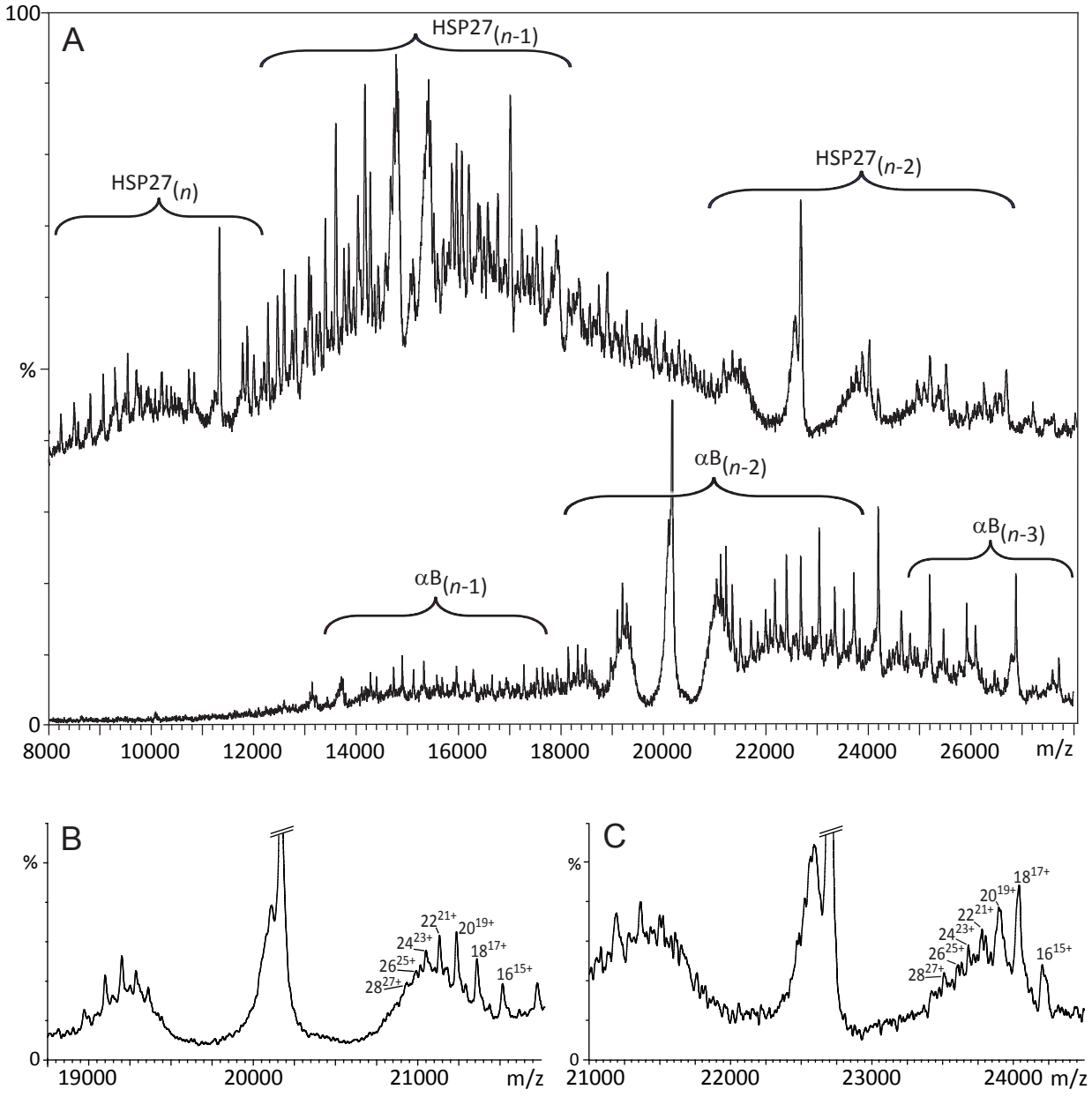
A
100
%
0
HSP27(n)
HSP27(n-1)
HSP27(n-2)
αB(n-1)
αB(n-2)
αB(n-3)
8000
10000
12000
14000
16000
18000
20000
22000
24000
26000
m/z
B
%
0
19000
20000
21000
m/z
22 21+
20 19+
24 23+
18 17+
26 25+
16 15+
28 27+
C
%
0
21000
22000
23000
24000 m/z
18 17+
20 19+
22 21+
24 23+
26 25+
28 27+
16 15+

Figure 4

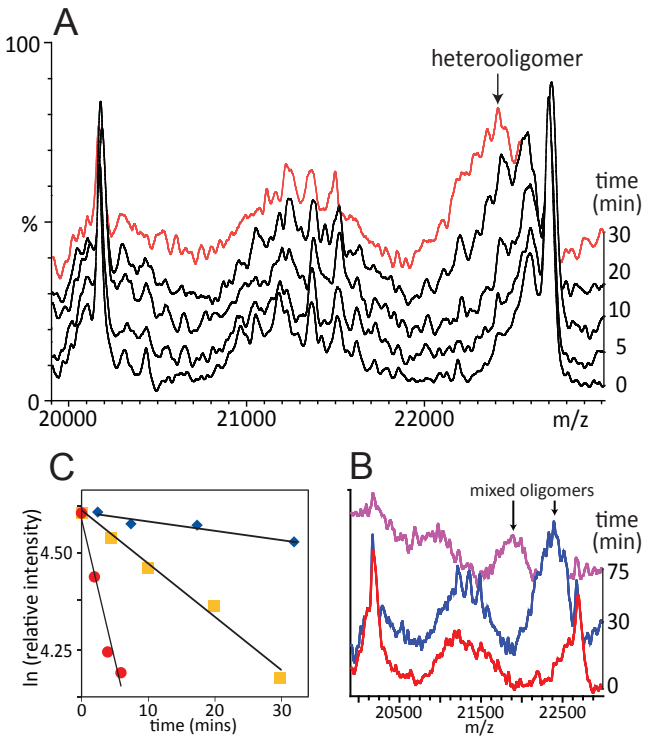
A
100
%
0
heterooligomer
time
(min)
30
20
10
5
0
20000
21000
22000
m/z
C
ln (relative intensity)
4.50
4.25
0
10
20
30
time (mins)
B
mixed oligomers
time
(min)
75
30
0
20500
21500
22500
m/z